ELSEVIER

European Journal of Pharmacology 419 (2001) 127–138

ejp

www.elsevier.nl/locate/ejphar

Effect of alisol B acetate, a plant triterpene, on apoptosis in vascular smooth muscle cells and lymphocytes

Huei-Wen Chen [a,b], Ming-Jen Hsu [b], Chiang-Ting Chien [a,*], Huei-Chen Huang [b]

[a] *Office for Medical Research, National Taiwan University Hospital, No. 7, Chung San South Road, Taipei, Taiwan*
[b] *Department of Pharmacology, College of Medicine, National Taiwan University, Taipei, Taiwan*

Received 4 April 2001; accepted 10 April 2001

Abstract

Glucocorticoid-induced apoptosis is a well-recognized physiological regulator of T-cell number and function. Alisol B acetate, a triterpene from *Alisma Plantago-aquatica*, has a glucocorticoid-like structure, and may have a similar function like glucocorticoid-induced apoptosis in both vascular smooth muscle cell line (A7r5) and human acute lymphoblastic leukemia cell line (CEM cells). For exploring its mechanism, mitochondria membrane potential and apoptosis-related gene expression were discussed. Alisol B (10^{-6}–10^{-4} M) inhibited serum-stimulated DNA synthesis in a concentration-dependent manner ($IC_{50} = 4.0 \pm 0.8 \times 10^{-6}$ M in A7r5 and $2.1 \pm 1.2 \times 10^{-6}$ M in CEM cells). The cell viability was reduced at 10^{-4} M of alisol B. Similar results were seen in dexamethasone treatment (a synthetic glucocorticoid, 10^{-6} M, 48 h). Apoptosis was induced after the cells were exposed to 10^{-5}–10^{-4} M alisol B or 10^{-6} M dexamethasone for 48 h. The mitochondrial membrane potential ($\Delta\Psi_m$) was significantly reduced after the alisol B treatment, indicating that the mitochondria might play a role in the alisol B induced cell apoptosis. Alisol B (10^{-5}–10^{-4} M) increased the levels of c-myc and bax mRNA and proteins, but not on the anti-apoptotic proto-oncogene, bcl-2, in A7r5 and CEM cells. In contrast, dexamethasone (10^{-6} M) treatment only caused significant increase in *c-myc* mRNA levels. These results suggest that the increased ratio of Bax/Bcl-2 and the decreased mitochondrial membrane potential might be involved in the mechanisms of alisol B-induced cell apoptosis. © 2001 Published by Elsevier Science B.V.

Keywords: Alisol B acetate; Apoptosis; A7r5 vascular smooth muscle cell; CEM lymphocyte; Mitochondria membrane potential

1. Introduction

The rhizome of *Alisma Plantago-aquatica*, used in various Chinese medicine preparations, has both hypolipidemic and anti-allergic effects (Imai et al., 1970; Kubo et al., 1997). *Alisma* rhizome contains active triterpenoids including alisol A, B and their related compounds (Imai et al., 1970). Triterpenoids have a variety of biological effects, such as anti-inflammatory, anti-hyperlipidemia, anti-ulcer, hepatoprotective, skin tumor prevention, and immunomodulatory effects (Mahato et al., 1988, 1992; Es-saady et al., 1996). However, the detailed mechanisms for triterpenoids on these biological effects are yet to be determined on cell physiology are still unclear. Since the triterpenoids have a common steroid-like structure, they are expected to have steroid-like pharmacological activities (Witkowski and Konopa, 1981; Lee et al., 1994). Glucocorticoid-induced apoptosis is a well-recognized process to regulate murine T-cell number and function (Brunetti et al., 1995). Whether the triterpene (alisol B) exerts a similar effect on cellular apoptosis is explored in this study.

Abnormal accumulation and proliferation in vascular smooth muscle cells and inflammatory mononuclear cells resulted to the pathogenesis of atherosclerosis and post-angioplasty restenosis (Lundergan et al., 1991; Ross, 1993). We have previously reported that certain plant phenols reduce the proliferative responses of vascular smooth muscle cells and/or mononuclear cells (Huang et al., 1992a,b, 1993, 1994a,b). We have also demonstrated that cucurmin, a plant phenol, induced cell apoptosis and also reduced cell proliferation (Chen and Huang, 1998). Recently, we found that alisol B acetate (Fig. 1), a plant triterpene, reduced cell proliferation and induced cell apoptosis in vascular smooth muscle cells and CEM lymphocytes.

Apoptosis (programmed cell death) plays a critical role in both the normal development and the pathology of a wide variety of tissues, and is characterized by cytoplasmic

* Corresponding author. Tel.: +886-2-2312-3456 ext. 5720; fax: +886-2-2394-7927.
E-mail address: ctchien@ha.mc.ntu.edu.tw (C.-T. Chien).

0014-2999/01/$ - see front matter © 2001 Published by Elsevier Science B.V.
PII: S0014-2999(01)00983-9

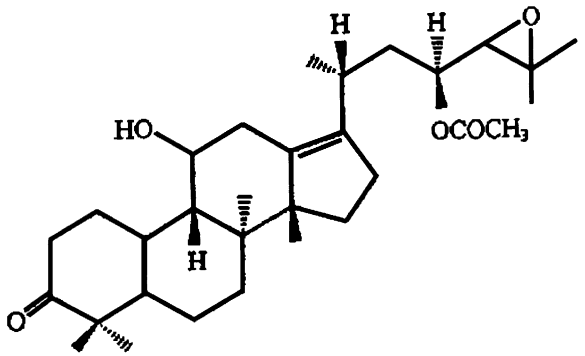

Fig. 1. Structures of alisol B monoacetate.

shrinkage, nuclear condensation and DNA fragmentation (Jacobson et al., 1997; Nagata, 1997). Initiation of apoptosis is controlled by regulation of the balance between the death and life signals perceived by the cell (Musci et al., 1997). In recent years, the regulation of cell cycle and apoptosis has received much attention as a possible means of eliminating excessively proliferative cells and it was, therefore, of interest to investigate the effects of alisol B on cell apoptosis.

The mitochondrion is the organelle that generates energy required for proper functioning of the eukaryotic cell, especially in the cardiac myocyte. The mitochondrial transmembrane potential ($\Delta\Psi_m$) developing from the asymmetric distribution of protons and ions on both sides of the inner mitochondrial membrane, and establishing a chemical (pH) and electric gradient, essential for mitochondrial function (Kroemer et al., 1997). Recent studies emphasized the critical role of mitochondria in apoptosis signaling (Kroemer et al., 1997; O'Rourke, 1999). Several lines of evidence indicated that mitochondria play a central role in triggering apoptosis. Because an early reduction of the $\Delta\Psi_m$, and concomitant release of the mitochondrial protein cytochrome *C*, which has been identified as the apoptosis-inducing factor-2 (Apaf-2) were found in cells undergoing apoptosis (Kroemer et al., 1997; Green and Reed, 1998; O'Rourke, 1999). In the cytosol, cytochrome *C* in combination with Apaf-1 activates caspase-9 (Apaf-3), which consequently leads to caspase 3 activation and DNA fragmentation (Haunstetter and Izumo, 1998). The function of the Bcl-2 family acts on mitochondria to stabilize membrane integrity, to regulate the opening of the megachannel (O'Rourke, 1999), and to protect cells from apoptosis. Evidence from our laboratory (Chen and Huang, 1998) confirmed the hypothesis that inhibition of bcl-2 mRNA expression by curcumin triggered the occurrence of cellular apoptosis.

The aim of this study was to determine whether an alteration in mitochondria function might contribute to alisol B-induced apoptotic cell death. One of the possible clinical applications of alisol B is to reduce the proliferation of both inflammatory cell and smooth muscle cell in atherosclerosis or post-angioplasty restenosis. Thus, alisol B may be useful in apoptotic therapy and as a valuable tool in the investigation of apoptotic progression.

2. Materials and methods

2.1. Cell lines

A7r5 cells (rat aortic smooth muscle cells) were grown in Dulbecco's Modified Eagle's medium supplemented with 10% v/v fetal calf serum, 100 μg/ml penicillin, and 1 μg/ml streptomycin. CEM cells (human CEM lymphocytes) were grown in RPMI-1640 medium containing 10% v/v fetal calf serum. Normal human polymorphonuclear leukocytes were freshly isolated from heparin-anticoagulated venous blood samples by centrifugation on the Ficoll-gradient. The polymorphonuclear leukocytes was collected and resuspended in Hank's balance salt solution with Ca^{2+} and Mg^{2+} (HBSS).

2.2. Measurement of DNA synthesis

DNA synthesis in A7r5 and CEM cells was determined by tritiated thymidine uptake (Huang et al., 1992b, 1994a). Prior to all experiments, confluent cells were rendered quiescent by 48-h culture (with one medium change after 24 h) in 0.5% v/v fetal calf serum instead of 10%. In A7r5 cells (10^4 cells/well) or CEM cells (5×10^3 cells/well), 10% v/v fetal calf serum and the test compound were added to the medium for 24 or 48 h. Then, 4 h before the end of time period, [^{3}H]thymidine (1 μCi/well) was added to the medium. At the end of the experiment, the cells were harvested and the incorporated [^{3}H]thymidine determined.

Each experiment was performed in triplicate and repeated five or six times. The inhibitory activity of the test compound is expressed as the percentage of serum-stimulated control value in the absence of test compound. The concentration causing 50% of the maximal inhibition (IC_{50}) was calculated for each experiment.

Cell viability was determined using the Trypan blue dye exclusion method. After addition of the test compound for 48 h, the cells were harvested, treated with trypan blue and the viability was determined by cell counting using a haemocytometer.

2.3. Flow cytometry analysis

Cells, synchronized at the G_0 phase by serum depletion for 48 h, were washed and then incubated in fresh medium containing 10% v/v fetal calf serum to allow them to progress through the cell cycle. At various time periods after release from the quiescent state, cell cycle distribution was analyzed by flow cytometry (Chen and Huang, 1998; Sherwood and Schimke, 1995). Following various treatments, A7r5 cells (10^6 cells/ml) were treated with

trypsin and RNase, then stained with propidium iodide (CycleTEST plus DNA reagent kit, Becton Dickinson, San Jose, CA). The samples were analyzed using a FACScan flow cytometer (Becton Dickinson), and the data was collected, stored, and analyzed using ModFit software (Becton Dickinson). Each experiment was repeated four to five times.

Apoptotic cells were also detected by both propidium iodide and Annexin V labeling as described, previously (Boersma et al., 1996; Zamai et al., 1996). Double-labeling was performed at 37°C as follows: propidium iodide (50 μg/ml) and Annexin V (2 μg/ml) were added to the culture medium for 2 h, and the staining was then immediately analyzed on a FACScan. Annexin V is a protein that binds to phosphatidylserine residues, which are exposed on the surface of apoptotic cells, but not on normal cells. In healthy cells, the distribution of the phosphatidylserine groups in the plasma membrane is asymmetrical with the groups being directed toward the interior of the cell. However, during apoptosis, this asymmetry is lost, and the phosphatidylserines are exposed to the exterior of the cell. Annexin V staining is, therefore, an established biochemical marker of apoptosis. The partial loss of membrane integrity or functionality is a useful criterion for distinguishing apoptotic from necrotic and living cells.

2.4. The terminal deoxynucleotidyl transferase-mediated dUTP nick end labeling (TUNEL) assay for apoptosis

Incorporation of modified nucleotides at free 3′-OH ends of DNA in cultured cells was modified from the method described by Gavrieli et al. (1992) and Chen and Huang (1998). Following treatment with the test compound, the cells were collected and plated on glass slides by Cytospin, then fixed with ice cold 95% v/v ethanol. The slides were rehydrated in phosphate-buffered saline (PBS) and incubated in 0.3% v/v H_2O_2 in water for 5 min to block endogenous peroxidase, and then the specimens were covered with terminal deoxynucleotidyl transferase (0.3 eu/μl) and biotinylated dUTP (10^{-3} M) in terminal deoxynucleotidyl transferase buffer containing 3×10^{-2} M Tris–HCl (pH 7.2), 1.4×10^{-1} M sodium cacodylate, and 10^{-3} M cobalt chloride for 1 h at 37°C. The reaction was terminated by Tris–buffered saline for 5 min at room temperature. The slides were covered with avidin/biotinylated peroxidase complex for 30 min and the peroxidase was visualized by using 3,3′-diaminobenzidine for 10 min. Counterstaining was performed with 5% methyl green in 10^{-1} M sodium acetate solution (pH 4.0) for 5 min, and the stained cells were analyzed under light microscopy. In each experiment, the negative control was treated with the label solution, but not with terminal transferase, and the positive control was exposed for 10 min at room temperature to DNase I (10^{-6} g/ml in 4×10^{-2} M Tris–HCl, 6×10^{-3} M $MgCl_2$, pH 7.5) prior to the TUNEL reaction.

2.5. DNA laddering

Cleavage of DNA into oligonucleosomal fragments, recognizable as a DNA ladder when electrophoresed on an agarose gel, is usually considered as the biochemical hallmark of apoptosis. Following treatment with the test compound, cells (10^7 cells/sample) were washed with PBS, and lysed in cell lysis buffer containing Tris, EDTA and sodium dodecyl sulphate. After the addition of RNase A (0.6 u/ml), the mixture was incubated at 37°C for 30 min. Protein precipitation solution (ammonium acetate) was added to the samples to eliminate protein contamination. Then the samples were centrifuged at 2000 *g* for 10 min. Cell lysates were treated with 100% isopropanol to precipitate DNA. The DNA pellet was washed with 70% v/v ethanol and dissolved in DNA hydration buffer containing Tris and EDTA. The DNA concentration was determined by spectrophotometry at 260 nm. Twenty micrograms of DNA was electrophoresed on a 1.0% w/v agarose gel containing 0.5 μg/ml of ethidium bromide. The DNA fragmentation bands were photographed under UV light and analyzed using an image analyzer (Winstar, Taiwan).

2.6. Analysis of mitochondrial membrane potential ($\Delta\Psi_m$)

Loss of $\Delta\Psi_m$ was assessed by fluorescence-activated cell sorter (FACS) analysis of cells stained with 5,5′,6,6′-tetrachloro-1,1′,3,3′-tetraethylbenzimidazolecarbocyanide iodide (JC-1). Cells were incubated with 10 μg/ml JC-1 (Molecular Probes), harvested, and analyzed by FACS (10,000 cells/sample). The excitation wavelength was 488 nm, and the JC-1 was monitored at 530 nm (FL1) and 582 nm (FL2). The data were analyzed using Cell Quest (Becton Dickinson, Immunocytochemistry Systems).

2.7. RT-PCR analysis of c-myc, bax and bcl-2 mRNA expression

Expression of *c-myc*, *bax* and *bcl-2* mRNA was analyzed by the reverse transcription-polymerase chain reaction (RT-PCR) technique (Chen and Huang, 1998; Huang et al., 1994a; Wang et al., 1989). Prior to RNA extraction, the confluent cells were rendered quiescent by culturing for 48 h in 0.5% v/v fetal calf serum instead of 10%, then the test compound together with 10% v/v fetal calf serum were added to the medium and incubated for the indicated time period. Total cellular RNA was prepared by acid guanidinium thiocyanate extraction (Chomczynski and Sacchi, 1987), and reverse transcribed into cDNA. Twenty microliters of reverse transcription reaction mixture containing 1 μg of total cellular RNA, 1 × PCR buffer (100 mM Tris–HCl, pH 8.3, 50 mM KCl), 0.3 mM deoxynucleoside triphosphates (dNTPs), 1 unit of RNase inhibitor, 2.5 μM of oligo$(dT)_{16}$, and 10 units of M-MLV reverse transcriptase was incubated at 42°C for 1 h, heated to 95°C for 5 min, and then quick-chilled at 5°C for 5 min. The

amounts of reverse-transcriptase products taken for PCR amplification of the test transcripts were within the range 0.5–5 μl. PCR was performed in a final volume of 100 μl in 1 × PCR buffer containing a final concentration of 0.5 μM each 3′ and 5′ primers and 2.5 unit of *AmpliTaq* DNA polymerase (Perkin-Elmer). The mixture was amplified for 35 cycles using a Perkin-Elmer thermal cycler (GeneAmp PCR System 9600), using an amplification profile of denaturation at 95°C for 15 s, annealing and extension at 65°C for 15 s. Primers for *c-myc*, *bax*, and *bcl-2* were used to generate 479, 371 and 235 bp fragments, respectively. The GAPDH primer (452 bp) was used as the internal standard. In each experiment, a negative control without reverse transcriptase was performed. Amplification products were separated by agarose gel electrophoresis and visualized by ethidium bromide staining. The gel was photographed with Polaroid type 667 film, and the digitized images were analyzed using an image analyzer (Winstar LV1, Taiwan). The signal intensity of the test genes were normalized to their respective GAPDH signal intensity and expressed in arbitrary units. The results were confirmed by Northern blotting using standard methods (Sambrook et al., 1989).

In a preliminary experiment, various aliquots taken from the RT reaction were subjected to PCR for analysis of the test transcripts, indicating that the amounts of cDNA produced were proportional to the inputs of the RT-PCR products over the range 0.5–5 μl. Thus, in subsequent experiments the amount of reverse-transcriptase products used for PCR amplification of the test transcripts was within this linear range to ensure that the amounts of cDNA produced truly reflected the levels of mRNA in the original samples.

2.8. Western blotting

Immunoblot analysis of protein expression was performed as described previously (Fadeel et al., 1999). Briefly, cell lysates were electrophoresed on 12% sodium dodecyl sulfate polyacrylamide gels (SDS-PAGE) under non-reducing conditions, and then electroblotted onto nitrocellulose membranes. Membranes were blocked in 1% bovine serum albumin and 5% non-fat dried milk, then incubated with primary antibodies specific for c-Myc, Bax, and Bcl-2 (1:100) and finally incubated with alkaline phosphatase-conjugated goat anti-mouse IgG antibody (1:10,000). Membranes were developed using, the substrate of alkaline phosphatase, nitro blue tetrazolium/5-bromo-4-chloro-3-indolyl phosphate (NBT/BCIT).

2.9. Materials

Alisol B acetate (Alisol B-23 monoacetate) (Fig. 1) was purchased from Nacalai Tesque (Kyoto, Japan). Rat aortic smooth muscle cells (A7r5 cells) and human CEM lymphocytes (CEM cells; human lymphoblastoid leukemia cells) were purchased from the American Type Culture Collection (Rockville, MD). Foetal calf serum, penicillin, streptomycin, Dulbecco's Modified Eagle's Medium (DMEM) and RPMI 1640 medium were purchased from Gibco Laboratories (Grand Island, NY). Thymidine [methyl-^{3}H] (5 Ci/mmol) was purchased from Amersham (Buckinghamshire, UK). Terminal deoxynucleotidyl transferase and biotinylated dUTP were purchased from Boehringer Mannheim Biochemicals (Indianapolis, IN). Avidin–peroxidase complex was purchased from Vector Laboratories (Burlingame, CA). Dexamethasone, 3,3-diaminobenzidine, nitro blue tetrazolium, and 5-bromo-4-chloro-3-indolyl phosphate were purchased from Sigma (St. Louis, MO). The in situ cell death detection kit, converter-POD (horseradish peroxidase-conjugated Fab fragment of sheep anti-fluorescein antibody), and Annexin-V-FLUOS (fluorescence-conjugated anticoagulant) were purchased from Boehringer Mannheim Biochemicals (Indianapolis, IN). The cycleTEST plus DNA reagent kit was purchased from the Becton Dickinson. The DNA isolation kit was purchased from Gentra systems (Research Triangle Park, NC). M-MLV (Moloney murine leukemia virus) reverse transcriptase and *AmpliTaq* DNA polymerase were purchased from Perkin-Elmer (Norwalk, CT). Primer for *bcl-2* (235 bp) was purchased from Maxim Biotech (So, San Francisco, CA), while the primers for *c-myc* (479 bp), *Bax* (371 bp), and GAPDH (452 bp) were purchased from Clontech Lab. (Palo Alto, CA). Primary antibodies specific for c-Myc, Bax, and Bcl-2 were purchased from Oncogene Research Products (Cambridge, MA) and the alkaline phosphatase-conjugated goat anti-mouse Ig antibody was purchased from Santa Cruz, CA, USA.

2.10. Statistical analysis

The data are expressed as mean ± S.E.M. *P*-values less than 0.05 were considered statistically significant (analysis of variance, ANOVA, and Student's *t* test).

3. Results

3.1. Effect on DNA synthesis

DNA synthesis was studied by incorporation of [^{3}H]thymidine into cellular DNA. The control values for serum-stimulated [^{3}H]thymidine incorporation in A7r5 (10^4 cells/well) and CEM cells (5×10^3 cells/well) in the absence of test compound were 7266 ± 755 and 7031 ± 332 cpm/well, respectively. Exposure of A7r5 and CEM cells to alisol B (10^{-5}–10^{-4} M) for 48 h resulted in a significant concentration-dependent inhibition of serum-stimulated [^{3}H]thymidine incorporation (Fig. 2). The IC_{50} values of alisol B were 4.0 ± 0.8 and 2.1 ± 1.2 × 10^{-6} M in A7r5 and CEM cells, while the maximum inhibition values were 100.0 ± 10.3 and 95.3 ± 1.2% at 10^{-4} M in A7r5 and CEM cells. Alisol B reduced the [^{3}H]thymidine

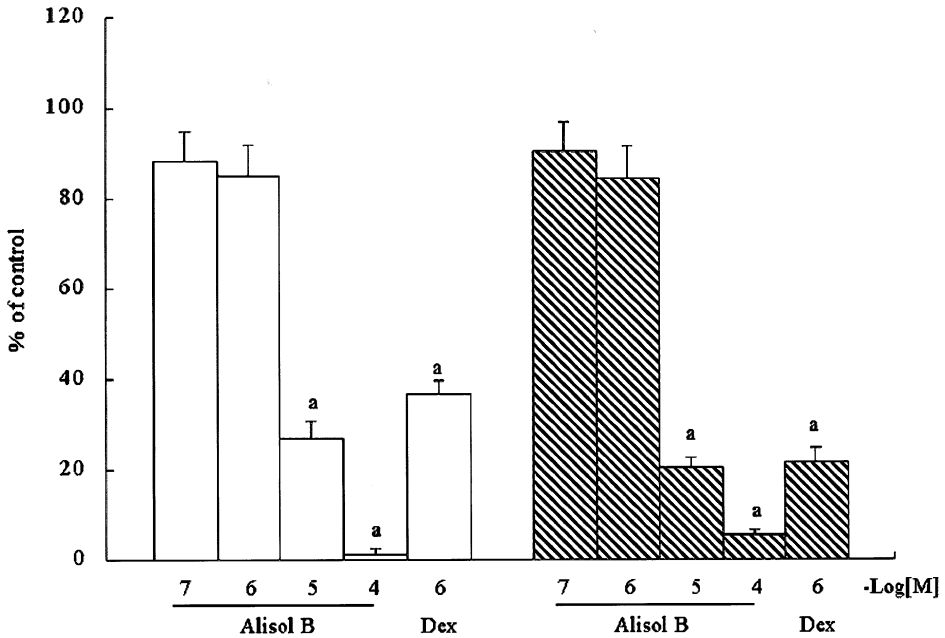

Fig. 2. Effects of alisol B on DNA synthesis in A7r5 (□) and CEM cells (▨). DNA synthesis was measured by uptake of tritiated thymidine. A7r5 cells (10^4 cells/well) (open column) and human CEM lymphocytes (5×10^3 cells/well) (filled column) were treated with alisol B or dexamethasone for 48 h. Control values for serum-induced [^{3}H]thymidine incorporation in the absence of test compound were 7266 ± 755 and 7031 ± 332 cpm/well for A7r5 and CEM cells, respectively. Inhibitory activities of the test compound are expressed as a percentage of the control values (% of control). Each column with vertical line represents the mean ± S.E.M. ($n = 5$). [a] $P < 0.05$, compared to control values in the absence of test compound.

incorporation of two cell lines to a similar extent. In this study, dexamethasone (10^{-6} M) inhibited the serum-stimulated [^{3}H]thymidine incorporation by 61.7 ± 4.5% and 76.3 ± 2.4% in A7r5 and CEM cells, respectively (Fig. 2).

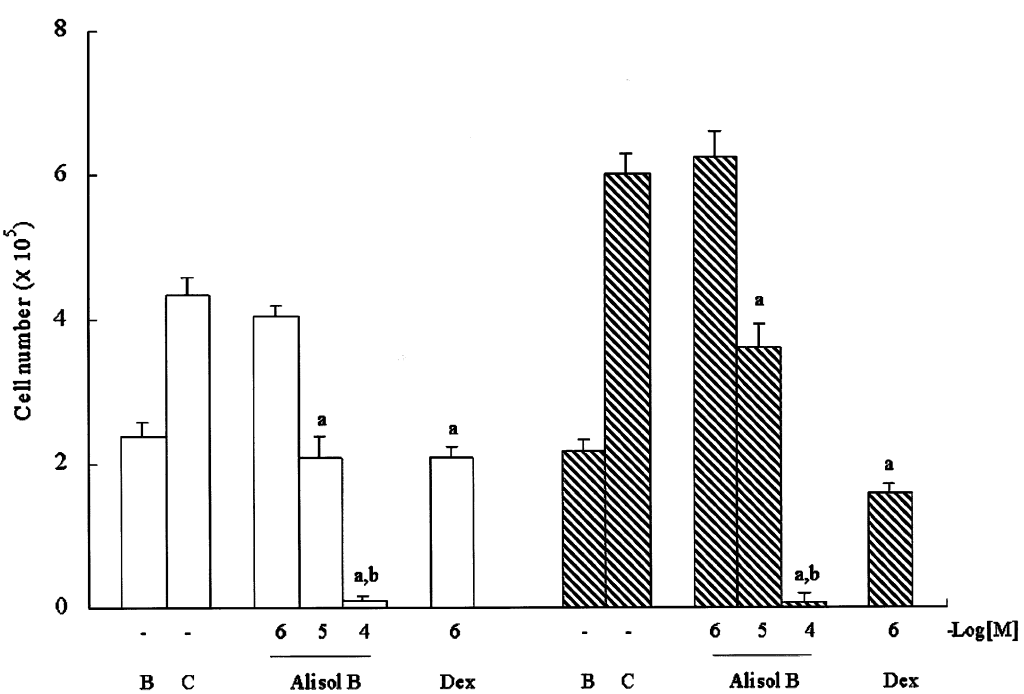

Fig. 3. Effect of alisol B on A7r5 (□) and CEM cells (▨) growth. Quiescent A7r5 and CEM cells (2×10^5 cells) were stimulated with serum. After addition of serum for 48 h in the absence (control level) or presence of test compound, the cells were harvested and their viability examined by Trypan blue exclusion test. The number of viable cells was estimated using a haemocytometer. Each column represents the mean ± S.E.M. ($n = 5$). [a] $P < 0.05$, compared with control cell numbers. [b] $P < 0.05$, compared with basal cell numbers (basal level, 2×10^5).

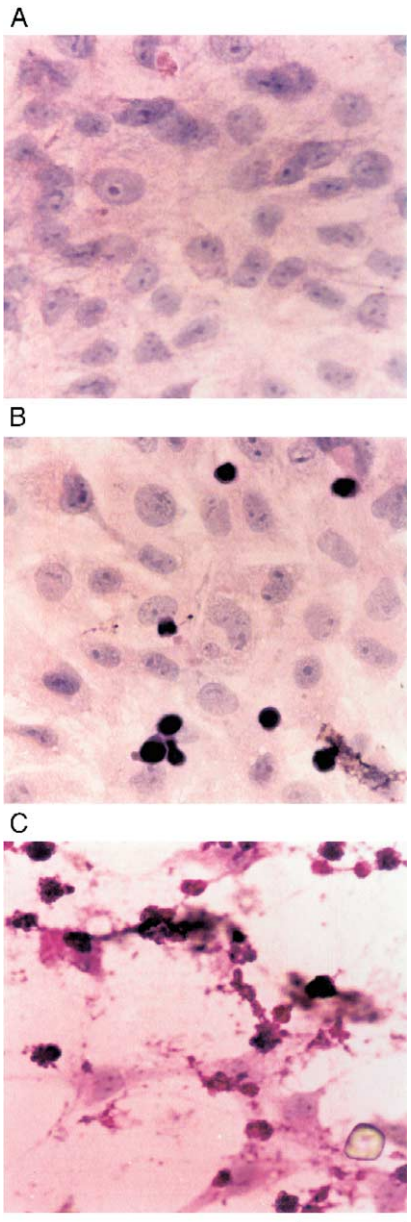

Fig. 4. Morphology of control and alisol B-treated A7r5 cells. Exponentially growing A7r5 cells cultured in cover slides were treated with or without alisol B. After 48 h, cells were fixed and stained with haematoxylin and eosin to examine the morphological changes. (A) Control (untreated); (B) 10^{-5} M alisol B, (C) 10^{-4} M alisol B. Bar = 30 μm. Similar results were obtained in three independent experiments.

3.2. Cell viability

As shown in Fig. 3, cell viability as determined by Trypan blue exclusion, was not affected by alisol B at concentrations lower than 10^{-5} M ($n = 5$) and the number of viable cells was greater than the basal value (2×10^5 cells). However, 10^{-4} M alisol B significantly reduced cell viability ($n = 5$). In freshly isolated human polymorphonuclear leukocytes, the cell viability was reduced to 84.3% after 48 h-cultured. When the polymorphonuclear leukocytes cells were treated with alisol B, the cell viability was not reduced significantly below the concentration of 10^{-5} M ($91.2 \pm 5.3\%$ at 10^{-6} M and $84.2 \pm 8.3\%$ at 10^{-5} M alisol B, compared with control, $P > 0.05$), but significantly reduced at 10^{-4} M ($39.8 \pm 3.1\%$, $P < 0.05$). These results indicating that alisol B has no cell cytotoxicity at concentrations lower than 10^{-5} M, although not at 10^{-4} M in normal human polymorphonuclear leukocytes. In this study, dexamethasone (10^{-6} M) also significantly reduced the numbers of viable cells in CEM cells ($n = 5$), but not in A7r5 cells.

3.3. Apoptosis

Cell apoptosis was induced in both A7r5 and CEM cells by a 4-h treatment with 10^{-4} M alisol B and 48-h treatment with 10^{-5} M alisol B. Some cells shrank and retracted from neighboring cells. Cytoplasm condensation was observed, and a lot of blebbed apoptotic bodies were found. Some surviving cells also showed certain degrees of morphological change, with an elongated and bipolar appearance (Fig. 4). The alisol B-induced apoptosis was characterized by flow cytometry (propidium iodide/annexin-V), terminal deoxynucleotidyl transferase-mediated dUTP nick end labeling (TUNEL) analysis, and DNA laddering.

The percentage of apoptotic cells following treatment with the test compound was analyzed by flow cytometry. Table 1 shows the concentration-dependent effect of alisol B treatment in inducing apoptosis. Following 48-h treatment with 10^{-5} M alisol B, the percentage of cells in the apoptotic region (Ap, sub-G_0/G_1 peak, subdiploid peak) increased significantly to 22.3 ± 4.7 and $18.3 \pm 3.7\%$ ($n = 5$) for A7r5 and CEM cells, respectively (Table 1). Using 10^{-4} M alisol B, the percentage of cells in the apoptotic region increased to $78.3 \pm 8.7\%$ in A7r5 cells and $69.7 \pm 6.8\%$ in CEM cells ($n = 5$) (Table 1). In this study, 10^{-6} M dexamethasone also caused a significant increase in the percentage of cells in the apoptotic region to $23.3 \pm 4.1\%$ in A7r5 cells, and $34.1 \pm 1.9\%$ in CEM

Table 1
Percentage of apoptosis in A7r5 and CEM cells treated with alisol B or dexamethasone for 48 h
Values are mean ± S.E.M. for triplicate experiments.

	Concentration (M)	n	Apoptosis (%)	
			A7r5 cells	CEM cells
Control	–	7	5.9 ± 3.2	6.8 ± 1.4
Alisol B	10^{-6}	5	7.7 ± 2.4	7.7 ± 1.9
	10^{-5}	5	$22.3 \pm 4.7^{a,b}$	$18.3 \pm 3.7^{a,b}$
	10^{-4}	5	$78.3 \pm 8.7^{a,c}$	$69.7 \pm 6.8^{a,c}$
Dexamethasone	10^{-6}	5	23.3 ± 4.1^{a}	34.1 ± 1.9^{a}

[a] $P < 0.05$, when compared to the control value without test compounds.
[b] $P < 0.05$, when compared to 10^{-6} M alisol B treatment.
[c] $P < 0.05$, when compared to 10^{-5} M alisol B treatment.

cells ($n = 5$). Furthermore, analysis of the cell cycle distribution of A7r5 and CEM cells by flow cytometry showed that there was no significant change after 48-h exposure to alisol B (10^{-5}–10^{-4} M).

We used also supravital exposure to propidium iodide and Annexin V labeling for the detection of apoptosis, and Annexin V^+ propidium $iodide^+$ (upper right quadrant) or Annexin V^+ propidium $iodide^-$ (lower right quadrant) was always found (Fig. 5A). The 10^{-5}–10^{-4} M alisol B-treated cells were mainly Annexin V^+, and displayed two levels of labeling: the Annexin V^+ cells remained propidium $iodide^-$, corresponding to the early apoptotic cells and the Annexin V^+ cells were also propidium $iodide^+$, corresponding to advanced apoptotic cells and to necrotic cells. Our results demonstrate that alisol B caused membranous integrity loss after 4 h-treatment at the concentration range of 10^{-5}–10^{-4} M, and subsequently induced both apoptosis and necrosis.

The TUNEL procedure stains nuclei that contain nicked DNA, a characteristic of cells in the early stages of apoptotic cell death. This process was applied to cells treated in various ways, and results representative of three experiments are shown in Fig. 5B. Untreated cells and cells treated for 48 h with 10^{-6} M alisol B were negative for TUNEL staining, whereas the cells with nuclei not stained with TUNEL (TUNEL-negative, green-colored)

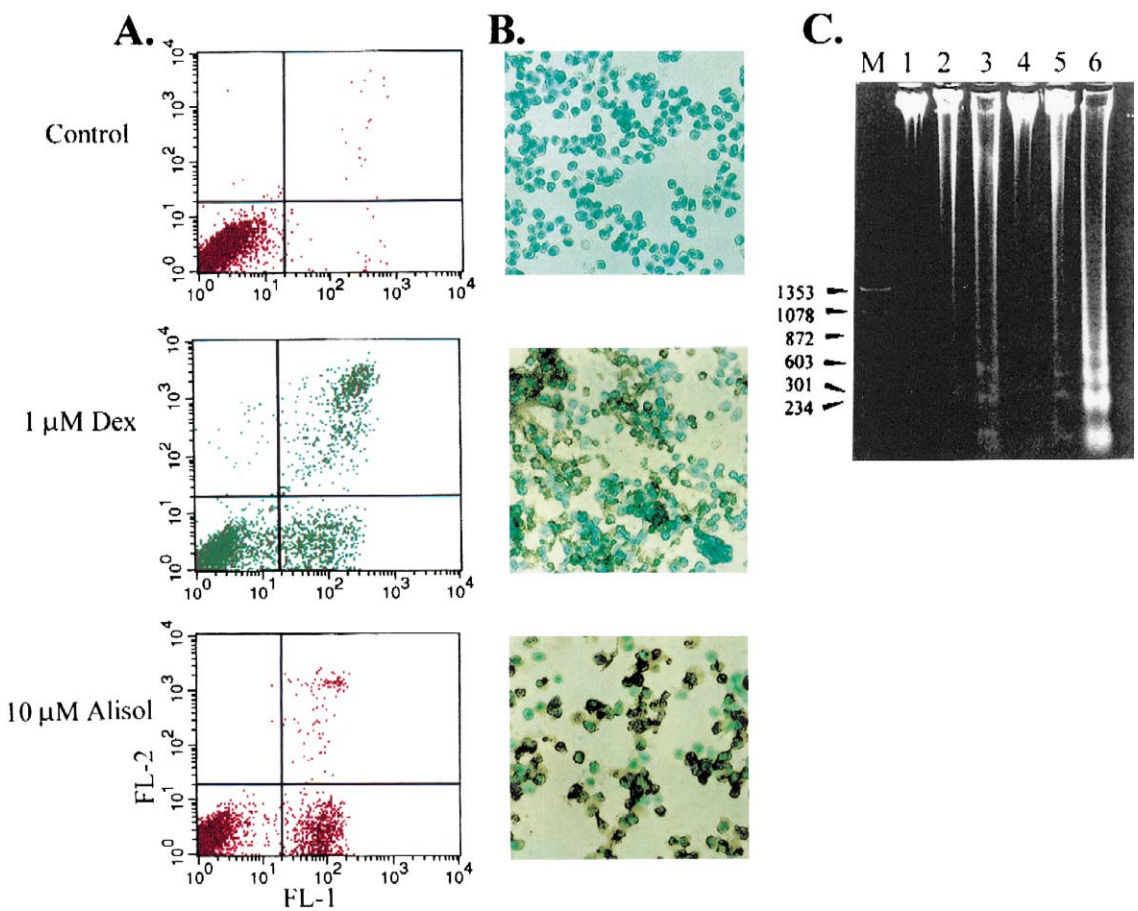

Fig. 5. (A) Contour diagram of Annexin V/propidium iodide flow cytomery. CEM cells, both untreated and treated with either 10^{-6} M dexamethasone or 10^{-5} M alisol B, were perfomed propidium iodide and Annexin V labeling as described in Section 2. The lower left quadrant of each panel (Annexin V^- propidium $iodide^-$) shows the viable cells, which exclude propidium iodide and are negative for Annexin V binding. The lower right quadrants (Annexin V^+ propidium $iodide^-$) represent the early apoptotic cells, Annexin V positive and propidium iodide negative, demonstrating cytoplasmic membrane integrity. The upper right quadrants (Annexin V^+ propidium $iodide^+$) contain advanced apoptotic cells and necrotic cells, positive for Annexin V binding and for propidium iodide uptake. (B) TUNEL analysis of CEM cells treated with alisol B. Using a peroxidase–substrate system, TUNEL-positive cells were visualized as having brown nuclei, while methyl green counter-staining showed green-blue nuclei. None of the nuclei in untreated cells were positively labeled for DNA fragmentation (upper), while a large proportion of the nuclei in 10^{-6} dexamethasone (Dex, middle) and 10^{-5} M alisol B-treated cells (below) were TUNEL-positive. Bar = 30 μm. Similar results were obtained in three independent experiments. (C) Electrophoresis of fragmented DNA in CEM cells treated with alisol B. Genomic DNA was isolated from CEM cells, either untreated (control) or treated with alisol B or dexamethasone for 48 h. DNA fragmentation was evaluated by electrophoresis on agarose gel containing ethidium bromide which was photographed under UV light. The DNA ladder was detected in cells treated with 10^{-5} and 10^{-4} M alisol B. The effect of test compound was compared to that of 10^{-6} M dexamethasone. Lane M, φX174/*Hae*III DNA size marker; lane 1, untreated control.; lane 2, treated with 10^{-7} M dexamethasone; lane 3, treated with 10^{-6} M dexamethasone; lane 4, treated with 10^{-6} M alisol B; lane 5, treated with 10^{-5} M alisol B; lane 6, treated with 10^{-4} M alisol B. Similar results were obtained in three independent experiments.

were visualized by counter-staining with methyl green. In contrast, following 48-h treatment with higher concentrations of alisol B (10^{-5} M), a large number of TUNEL-positive (brown) cells were seen (Fig. 5B), the stain being localized in the nuclei. TUNEL-positive cells were also seen following treatment for 48 h with 10^{-6} M dexamethasone (Dex).

Degradation of DNA into a specific fragmentation pattern is a characteristic feature of apoptosis. In contrast to the random fragmentation associated with necrosis, apoptosis-associated DNA fragmentation is characterized by cleavage of the DNA at regular intervals, visualized on agarose gel electrophoresis as a DNA ladder consisting of multimers of approximately 200 bp. After 48-h exposure to

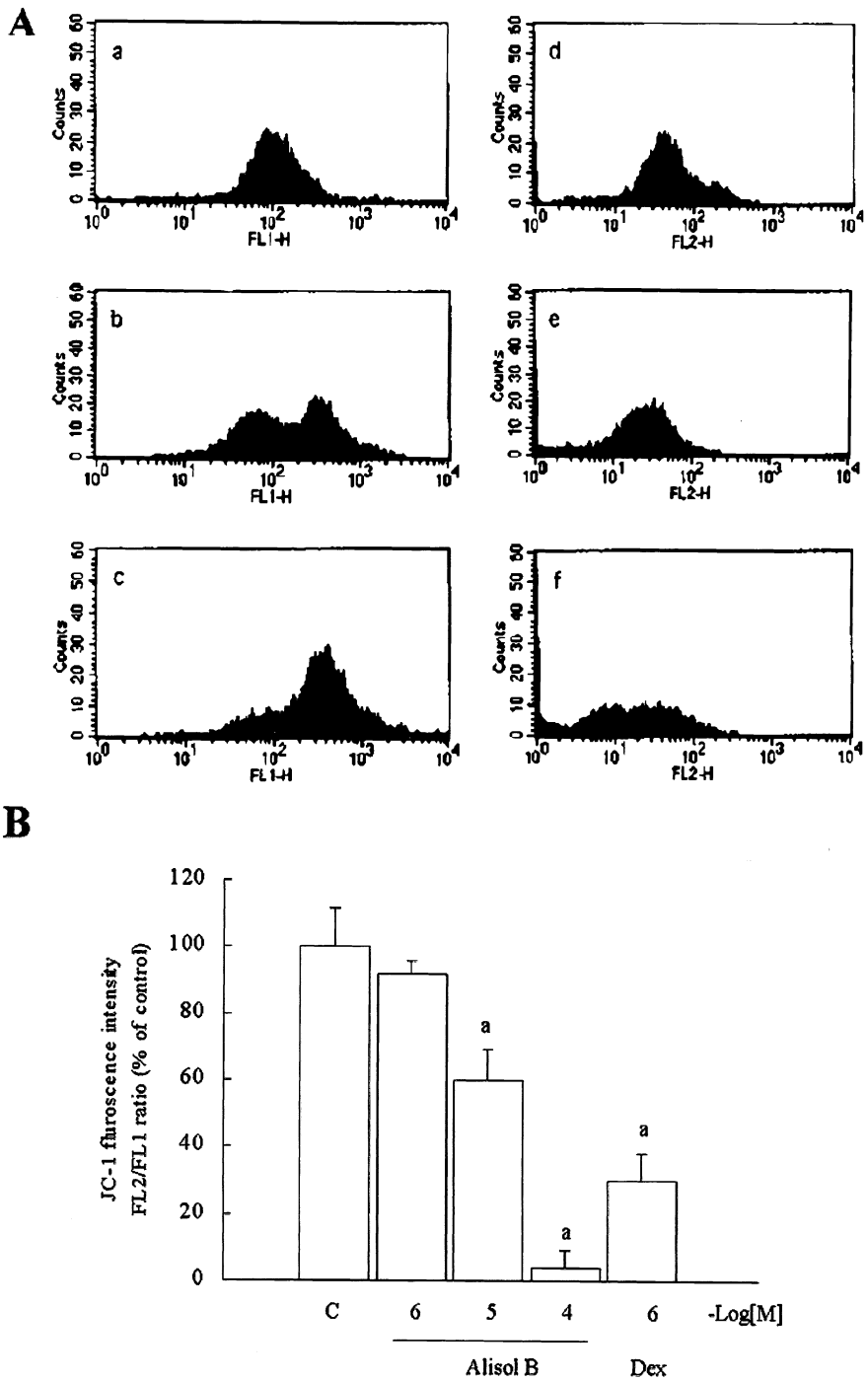

Fig. 6. Loss of mitochondrial membrane potential ($\Delta\Psi_m$) induced by alisol B (JC-1 FACS analysis). A7r5 cells were treated with alisol B (10^{-5}–10^{-4} M), stained with JC-1, and analyzed as described in Section 2. (A) (a, d) Untreated A7r5 cells; (b, e) A7r5 cells treatment with 10^{-5} M alisol B for 24 h; (c, f) A7r5 cells treatment with 10^{-4} M alisol B for 24 h. (B) JC-1 fluorescence intensity, FL2/FL1 ratio. The reduction of FL2/FL1 ratio was indicated that the $\Delta\Psi_m$ was lost. Data are expressed as mean ± S.E.M. ($n = 3$). [a] $P < 0.05$, compared with the untreated cells.

alisol B or dexamethasone, the genomic DNA from cells was subjected to agarose gel electrophoresis. Fig. 5C shows a representative result from three experiments. A clear DNA fragmentation ladder can be seen in CEM cells treated with 10^{-4} M alisol B (Fig. 5C, lane 6), but it was unclear in A7r5 cells (data not shown). This effect was much less apparent in cells treated with 10^{-5} M alisol B or 10^{-6} M dexamethasone (Fig. 5C, lanes 5, 3).

3.4. Loss of $\Delta\Psi_m$ in cells treated with alisol B

To determine if early loss of $\Delta\Psi_m$ occurred during alisol B treatment, we used an alternative fluorophore, JC-1, which can concentrate in mitochondria. It exists as monomers (green fluorescent, Em = 530 nm, FL-1) at lower mitochondrial membrane potential, and as red fluorescent J-aggregates (Em = 585 nm, FL-2) at higher membrane potential. In untreated cells, J-aggregates were accumulated in the mitochondria, but in alisol B-treated cells, JC-1 monomers were distributed in cells, as $\Delta\Psi_m$ was lost. This is associated with an increase in fluorescence intensity at 530 nm (FL-1) and a decrease in fluorescence at 585 nm (FL-2), when $\Delta\Psi_m$ was lost (Fig. 6A). The FL2/FL1 ratio may correlate more closely with $\Delta\Psi_m$ than with the only measurement of FL1 or FL2 fluorescence. Both the alisol B (10^{-5}–10^{-4} M) and dexamethasone (10^{-6} M) significantly reduced the FL2/FL1 ratio ($P < 0.05$), indicating that there was potential loss of mitochondrial membrane (Fig. 6B).

3.5. Effects on c-myc, bax, and bcl-2 expression

The *c-myc*, *bax*, and *bcl-2* mRNA levels in serum-stimulated A7r5 and CEM cells, either untreated or treated with test compound, were measured using the RT-PCR technique. The signal intensities for the test genes and

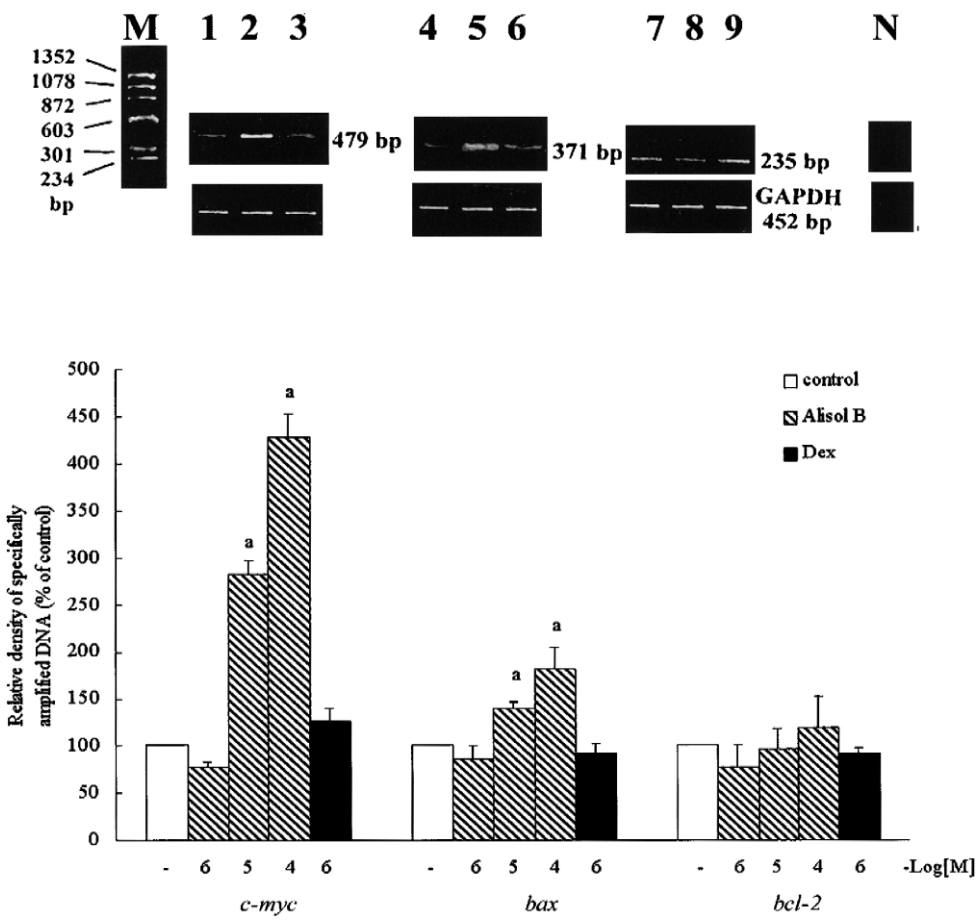

Fig. 7. Effects of alisol B on *c-myc*, *bax*, and *bcl-2* mRNA levels in A7r5 cells. Quiescent cells were stimulated by serum in the absence or presence of the test compound for 24 h. The serum-stimulated test gene mRNA levels in untreated cells (control) and those treated with 10^{-5} M alisol B or 10^{-6} M dexamethasone were analyzed by RT-PCR amplification as described in Section 2. Amplification products were separated by agarose gel electrophoresis and visualized by ethidium bromide staining. Signal intensities for the test genes and GAPDH were quantified using image analyzer, and the changes in the signal intensities of test genes relative to that for GAPDH were calculated. The results are expressed as a percentage of the control level in the absence of test compound (% of control) (bottom of figure) ($n = 3$); the corresponding electrophoretic patterns of PCR products are shown at the top of each panel. Lane M, φX174/*Hae*III DNA size marker; lanes 1, 4, 7, control; lanes 2, 5, 8, 10^{-5} M alisol B-treated; lanes 3, 6, 9, 10^{-6} M dexamethasone-treated. *c-myc* mRNA levels: lanes 1, 2, 3; *bax* mRNA level: lanes 4, 5, 6; *bcl-2* mRNA level: lane 7, 8, 9; lane N, negative control, no RT. Each column in the bottom part of the figure represents the mean ± S.E.M. ($n = 3$). [a] $P < 0.05$, compared with the control.

GAPDH were quantified using image analyzer (Fig. 7). The changes in the signal intensity of the test genes relative to GAPDH are shown at the bottom of Fig. 7. All three genes were expressed in A7r5 and CEM cells in the presence of serum. In a preliminary experiment, the effect of alisol B on the expression of *c-myc* and *bax* mRNA was found to be maximal at 24 h, and this time-point was, therefore, used in subsequent studies. After addition of alisol B (10^{-5} M) to A7r5 cells, the level of *c-myc* mRNA was significantly increased (2.9 ± 0.5-fold increase) (Fig. 7, lane 2, left filled column; $n = 3$), as was the level of *bax* mRNA (1.4 ± 0.1-fold increase) (Fig. 7, lane 5, center filled column; $n = 3$). However, the level of *bcl-2* mRNA was not significantly altered (1.0 ± 0.1-fold increase) (Fig. 7, lane 8, right filled column; $n = 3$). In the same cells, treatment with dexamethasone (10^{-6} M, 24 h) resulted in slight increases in *c-myc* mRNA levels and reductions in *bcl-2* mRNA levels (Fig. 7; lanes 3, 6 and 9), hatched columns; $n = 3$), although these changes did not achieve statistical significance. Similar results were also seen in the experiments using CEM cells. Addition of alisol B (10^{-5} M) resulted in a significant increase in the levels of *c-myc* mRNA (1.4 ± 0.1-fold increase) and *bax* mRNA (1.3 ± 0.08-fold increase), although the level of *bcl-2* mRNA was not significantly altered (0.9 ± 0.02-fold increase). The ratio of Bax/Bcl-2 increased significantly after the alisol B treatment (144.4% of control). Dexamethasone (10^{-6} M, 24 h) caused a slight induction in *c-myc* and reduction in *bcl-2* mRNA levels. However, the changes did not achieve statistical significance. The effects of alisol B on the mRNA levels were confirmed by Northern blotting. The protein levels of c-Myc and Bax were also significantly increased after alisol B (10^{-5} M) treatment (Fig. 8).

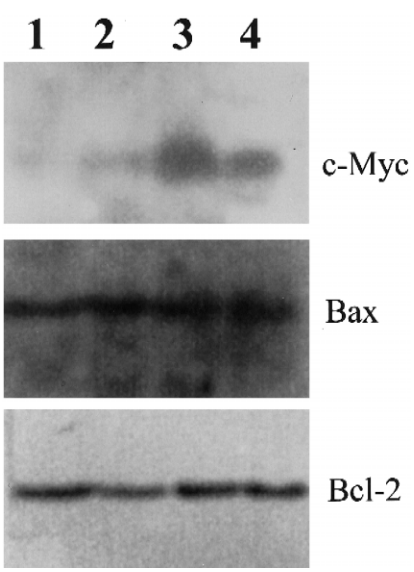

Fig. 8. The levels of c-Myc, Bax, and Bcl-2 protein expression were analyzed after the treatment of 10^{-5} M alisol B at the indicated time by Western blot assay using the specific monoclonal antibodies as indicated in Section 2. Lane 1, cells in the basal condition; lane 2, 10^{-5} M alisol B-treated for 24 h; lane 3, 10^{-4} M alisol B-treated for 24 h; lane 4, 10^{-6} M dexamethasone-treated for 24 h. Similar results were obtained in three independent experiments.

4. Discussion

The present results demonstrate for the first time that alisol B (alisol B acetate) inhibits cell proliferation and induces cell apoptosis in both rat aortic smooth muscle cells (A7r5 cells) and human CEM lymphocytes (CEM cells), which are important in the pathogenesis of atherosclerosis and restenosis. Thus, alisol B may, therefore, be useful in the study and treatment of these conditions. A cell viability test verified that the effects of alisol B were not due to general cellular toxicity.

As a process of normal or physiological cell death, apoptosis retaining cell intact and causing little inflammation may counteract mitosis and limit cells accumulation, and consequently inhibits intimal thickening, a key event in the pathogenesis of atherosclerosis and restenosis. Recent evidence suggests that the failure of cells to undergo apoptotic cell death may be involved in the pathogenesis of a variety of human diseases, including cancer, autoimmune diseases, and viral infections. Thus, specific therapies designed to enhance the susceptibility of individual cell types to undergo apoptosis could form the basis for treatment of a variety of human diseases (Thompson, 1995).

We have previously reported that the apoptotic effect of curcumin, a plant phenol, may be partly mediated by a reduction in *c-myc* and *bcl-2* mRNA expression (Chen and Huang, 1998). Some studies indicate that Bcl-2 family (Bcl-2 and Bax) play an important role in the apoptotic pathway (Hale et al., 1996; Schendel et al., 1998). The present results indicate that the levels of *c-myc* and *bax* mRNA were significantly increased in both vascular smooth cells and lymphocytes in the presence of alisol B, but no significant change was seen in *bcl-2* mRNA levels. That alisol B enhanced expression of *c-myc* and *bax* mRNA may partly contribute to cell apoptosis. In mammalian cells, Myc is a central regulator in cell cycle and induces cells to undergo apoptosis. Recent progress has shed light both on the factors regulating the function and expression of Myc and on the downstream targets in the cell cycle and suggests the existence of a novel signal transduction pathway regulating both apoptosis and proliferation (Desbarats et al., 1996). On the other hand, evidence suggests that the ratio of Bax/Bcl-2 can regulate the mitochondrial membrane potential and cytochrome *C* release. In the present study, alisol B (10^{-5} M) caused a significant loss of mitochondrial membrane potential and increase in *bax/bcl-2 ratio*, indicating that alisol B-induced apoptosis may be partly mediated via Bax/Bcl-2-regulated mitochondria pathway.

Since alisol B has a common steroid-like structure, it is expected that alisol B has some steroid-related pharmaco-

logical activities, such as glucocorticoid-induced apoptosis in murine T cell number and function (Brunetti et al., 1995). In this study, the apoptotic effect of alisol B was compared with that of dexamethasone, which causes down-regulation of the expression of the apoptosis-suppressing gene, *bcl-2*, and the apoptosis-promoting gene, *bax*, as well as up-regulation of the expression of the apoptosis-suppressing gene, *bcl-XL* (Lotem and Sachs, 1995) in M1 myeloid leukaemia cells. In our results, the changes in *c-myc*, *bax*, and *bcl-2* expressions induced by dexamethasone (10^{-6} M) did not achieve significance, implying that dexamethasone may have a different mechanism of action in these two cells.

The structural homology of the triterpenes with sterols raises another possibility that triterpenes may interact with the components of biological systems, primarily with sterols comprising the structure of biomembranes (Anisimov, 1987), causing disturbances in the selective permeability of the plasma membrane. Triterpenes affect the ionic permeability of liposomes and flat bilayer lipid membranes, and the rate at which they exert their effect depends on the quantitative and qualitative sterol level in the membrane (Anisimov, 1987). The steroid-like structure in alisol B may, in part, act through a receptor pathway (Evans, 1988), because triterpenes may regulate the expression of differentiation-specific genes, probably by forming a complex with the glucocorticoid receptor or its analogous nuclear receptor (Lee et al., 1994). The tetracyclic triterpenoid, cucurbitacin, has been reported to act on an unidentified target, leading to inhibition of macromolecule biosynthesis (Witkowski et al., 1984). This effect involves a mechanism resembling the immediate extragenomic effects of glucocorticoids which are not necessarily receptor-mediated.

In summary, our results indicate that alisol B-induced cell apoptosis may be partly via inducing c-Myc expression and Bax/Bcl-2-mediated mitochondrial membrane potential collapse. In addition to the apoptotic effect, it exhibits hypolipidemic activities and anti-inflammatory effects (Mahato et al., 1988, 1992). These results suggest that alisol B may be useful for the development of drugs to prevent the pathological changes associated with atherosclerosis and post-angioplasty restenosis. In the treatment of atherosclerosis and restenosis, a dose range of antiproliferative or apoptotic-inducing agent that can slow down the overdrive response of cell division without having a deleterious effect on the stability of atherosclerotic plaques should be used.

Acknowledgements

This investigation was supported by grants from the National Science Council, Taiwan, the Department of Health and the National Taiwan University Hospital (NTUH89A014 and NTUH89A023-10).

References

Anisimov, M.M., 1987. Triterpene glycosides and the structural–functional properties of membranes. Biol. Nauki 10, 49–63.

Boersma, A.W.M., Nooter, K., Oostrum, R.G., Stoter, G., 1996. Quantification of apoptotic cells with fluorescein isothiocyanate-labeled Annexin V in Chinese hamster ovary cell cultures treated with cisplatin. Cytometry 24, 123–130.

Brunetti, M., Martelli, N., Colasante, A., Plantelli, M., Muslani, P., Aiello, F.B., 1995. Spontaneous and glucocorticoid-induced apoptosis in human mature T lymphocytes. Blood 86, 4199–4205.

Chen, H.W., Huang, H.C., 1998. Effect of curcumin on cell cycle progression and apoptosis in vascular smooth muscle cells. Br. J. Pharmacol. 124, 1029–1040.

Chomczynski, P., Sacchi, N., 1987. Single-step method of RNA isolation by acid guanidinium thiocyanate–phenol chloroform extraction. Anal. Biochem. 162, 156–159.

Desbarats, L., Schneider, A., Muller, D., Burgin, A., Eilers, M., 1996. Myc: a single gene controls both proliferation and apoptosis in mammalian cells. Experientia 52, 1123–1129.

Es-saddy, D., Simon, A., Jayat-vignoles, C., Chulla, A.J., Delage, C., 1996. MCF-7 cell cycle arrested at G1 through ursolic acid, and increased reduction of tetrazolium salts. Anticancer Res. 16, 481–486.

Evans, R.M., 1988. The steroid and thyroid hormone receptor superfamily. Science 240, 889–895.

Fadeel, B., Orrenius, S., Henter, J.I., 1999. Induction of apoptosis and caspase activation in cells obtained from familial haemophagocytic lymphohistiocytosis patients. Br. J. Haematol. 106 (2), 406–415.

Gavrieli, Y., Sherman, Y., Ben-sasson, S.A., 1992. Identification of programmed cell death in situ via specific labeling of nuclear DNA fragmentation. J. Cell Biol. 119, 493–501.

Green, D.R., Reed, J.C., 1998. Mitochondria and apoptosis. Science 281, 1309–1312.

Hale, A.J., Smith, C.A., Sutherland, L.C., Stoneman, V.E., Longshorne, V.L., Culhane, A.C., Willams, G.T., 1996. Apoptosis: molecular regulation of cell death. Eur. J. Biochem. 236, 1–26.

Haunstetter, A., Izumo, S., 1998. Apoptosis: basic mechanisms and implications for cardiovascular disease. Circ. Res. 82, 1111–1129.

Huang, H.C., Huang, Y.L., Chang, J.H., Chen, C.C., Lee, Y.T., 1992a. Possible mechanism of immunosuppressive effect of scoparone (6,7-dimethoxycoumarin). Eur. J. Pharmacol. 217, 143–148.

Huang, H.C., Jan, T.R., Yeh, S.F., 1992b. Inhibitory effect of curcumin, an anti-inflammatory agent, on vascular smooth muscle cell proliferation. Eur. J. Pharmacol. 221, 381–384.

Huang, H.C., Lai, M.W., Wang, H.R., Chung, Y.L., Hsieh, L.M., Chen, C.C., 1993. Antiproliferative effect of esculetin on vascular smooth muscle cell: possible roles of signal transduction pathways. Eur. J. Pharmacol. 237, 39–44.

Huang, H.C., Hsieh, L.M., Chen, H.W., Lin, Y.S., Chen, J.S., 1994a. Effects of baicalein and esculetin on transduction signals and growth factors expression in T-lymphoid leukemia cells. Eur. J. Pharmacol., Mol. Pharmacol. Sect. 268, 73–78.

Huang, H.C., Wang, H.R., Hsieh, L.M., 1994b. Antiproliferative effect of baicalein, a flavonoid from Chinese herb, on vascular smooth muscle cells. Eur. J. Pharmacol. 251, 91–93.

Imai, Y., Matsumura, H., Aramaki, Y., 1970. Hypocholesterolemic effect of alisol A-24-monoacetate and its related compounds in rats. Jpn. J. Pharmacol. 20, 222–228.

Jacobson, M.D., Weil, M., Raff, M.C., 1997. Programmed cell death in animal development. Cell 88, 347–354.

Kroemer, G., Zamzami, N., Susin, S.A., 1997. Mitochondrial control of apoptosis. Immunol. Today 18, 44–51.

Kubo, M., Matsuda, H., Tomohiro, N., Yoshikawa, M., 1997. Studies on Alismatis rhizoma: I. Anti-allergic effects of methanol extract and six terpene components from Alismatis rhizoma (dried rhizome of Alisma orientale). Biol. Pharm. Bull. 20, 511–516.

Lee, H.Y., Chung, H.Y., Kim, K.H., Lee, J.J., Kim, K.W., 1994. Induc-

tion of differentiation in the cultured F9 teratocarcinoma stem cells by triterpene acids. J. Cancer Res. Clin. Oncol. 120, 513–518.

Lotem, J., Sachs, L., 1995. Regulation of bcl-2, bcl-XL and bax in the control of apoptosis by hematopoietic cytokines and dexamethasone. Cell Growth Differ. 6, 647–653.

Lundergan, C.F., Foegh, M.L., Ramwell, P.W., 1991. Peptide inhibition of myointimal proliferation by angiopeptin, a somatostatin analogue. J. Am. Coll. Cardiol. 17, 132B–136B.

Mahato, S.B., Sarkar, S.K., Poddar, G., 1988. Triterpenoid saponins. Phytochemistry 27, 3037–3067.

Mahato, S.B., Nandy, A.K., Roy, G., 1992. Triterpenoids. Phytochemistry 31, 2199–2249.

Musci, M.A., Latinis, K.M., Koretzky, G.A., 1997. Signaling events in T lymphocytes leading to cellular activation or programmed cell death. Clin. Immunol. Immunopathol. 83, 205–222.

Nagata, S., 1997. Apoptosis by death factor. Cell 88, 355–365.

O'Rourke, B., 1999. Apoptosis: rekindling the mitochondrial fire. Circ. Res. 85, 880–883.

Ross, R., 1993. The pathogenesis of atherosclerosis: a perspective for the 1990s. Nature 362, 801–809.

Sambrook, J., Fritsch, E.F., Maniatis, T., 1989. Molecular Cloning: A Laboratory Manual. Cold Spring Habor Laboratory, Cold Spring Habor, NY.

Schendel, S.L., Montal, M., Reed, J.C., 1998. Bcl-2 family proteins as ion-channels. Cell Death Differ. 5 (5), 372–380.

Sherwood, S.W., Schimke, R.T., 1995. Cell cycle analysis of apoptosis using flow cytometry. Methods Cell Biol. 46, 77–97.

Thompson, C.B., 1995. Apoptosis in the pathogenesis and treatment of disease. Science 267, 1456–1462.

Wang, A.M., Doyle, M.V., Mark, D.F., 1989. Quantitation of mRNA by the polymerase chain reaction. Proc. Natl. Acad. Sci. U. S. A. 86, 9717–9721.

Witkowski, A., Konopa, J., 1981. Binding of the cytotoxic and antitumor triterpenes, cucurbitacins, to glucocorticoid receptors of HeLa cells. Biochim. Biophys. Acta 674, 246–255.

Witkowski, A., Woynarowska, B., Konopa, J., 1984. Inhibition of the biosynthesis of deoxyribonucleic acid, ribonucleic acid and protein in HeLa S3 cells by cucurbitacins, glucocorticoid-like cytotoxic triterpenes. Biochem. Pharmacol. 33, 995–1004.

Zamai, L., Falcieri, E., Marhejka, G., Vitale, M., 1996. Supravital exposure to propidium iodide identifies apoptotic cells in the absence of nucleosomal DNA fragmentation. Cytometry 23, 303–311.